2014

Bottom-up solution synthesis of narrow nitrogen-doped graphene nanoribbons

Timonthy H. Vo
University of Nebraska-Lincoln

Mikhail Shekhirev
University of Nebraska-Lincoln

Donna A. Kunkel
University of Nebraska-Lincoln

François Orange
University of Puerto Rico

Maxime J. -F. Guinel
University of Puerto Rico

See next page for additional authors

ChemComm

COMMUNICATION

View Article Online
View Journal | View Issue

Bottom-up solution synthesis of narrow nitrogen-doped graphene nanoribbons†

Cite this: *Chem. Commun.*, 2014, **50**, 4172

Received 3rd February 2014,
Accepted 5th March 2014

DOI: 10.1039/c4cc00885e

www.rsc.org/chemcomm

Timothy H. Vo,[a] Mikhail Shekhirev,[a] Donna A. Kunkel,[b] François Orange,[c] Maxime J.-F. Guinel,[cd] Axel Enders[be] and Alexander Sinitskii*[ae]

Large quantities of narrow graphene nanoribbons with edge-incorporated nitrogen atoms can be synthesized *via* Yamamoto coupling of molecular precursors containing nitrogen atoms followed by cyclodehydrogenation using Scholl reaction.

Graphene nanoribbons (GNRs), narrow strips of graphene with high aspect ratios, attract a great deal of attention because of their interesting electronic and magnetic properties.[1] According to the theoretical studies, these properties strongly depend on the width of GNRs as well as their edge structure and termination, and are also very sensitive to the edge disorder.[2–5] Thus, it is very important to precisely control the structure of GNRs on the atomic scale. Numerous top-down fabrication approaches have been developed to produce GNRs from graphite, graphene or carbon nanotubes, as discussed in the recent review papers,[6–8] but the resulting ribbons typically have relatively large and non-uniform widths and disordered edges. Narrow atomically precise GNRs could be synthesized *via* bottom-up approaches that employ decomposition of molecules inside carbon nanotubes,[9,10] or rely on the surface-assisted[11–14] or solution polymerization[8,15–22] of molecular precursors followed by cyclodehydrogenation of the resulting polymers. While surface-assisted bottom-up synthesis of GNRs yields small quantities of ribbons on metallic substrates in ultrahigh vacuum conditions that are ideal for scanning tunnelling microscopy (STM) characterization, solution-based approaches are preferred for the bulk synthesis of GNRs, so these two groups of methods could be considered as complimentary.

Electronic properties of GNRs could be further tuned *via* their doping with heteroatoms, such as boron or nitrogen.[23] This possibility has been extensively studied theoretically,[24–30] but only a few experimental attempts to synthesize nitrogen-doped GNRs (N-GNRs) by bottom-up approaches have been reported.[14,20] Bronner *et al.* prepared chevron-like N-GNRs by the surface-assisted approach on Au(111) substrate and performed their spectroscopic characterization.[14] Kim *et al.* synthesized N-GNRs with a different structure in solution *via* Suzuki coupling of molecular precursors, one of which was dibrominated pyrazine, and cyclodehydrogenation of the resulting polymers.[20] Here we demonstrate that high-quality chevron-like N-GNRs could be synthesized *via* Yamamoto coupling of molecular precursors containing nitrogen atoms followed by cyclodehydrogenation *via* Scholl reaction (Fig. 1).

The structure of the N-GNR synthesized in this work is shown in Fig. 1a. Since the unit cell of this ribbon contains four nitrogen atoms, we refer to it as "4N-GNR". The monomer molecule **3** used as a precursor for the 4N-GNR synthesis is not symmetric relative to the plane perpendicular to the direction

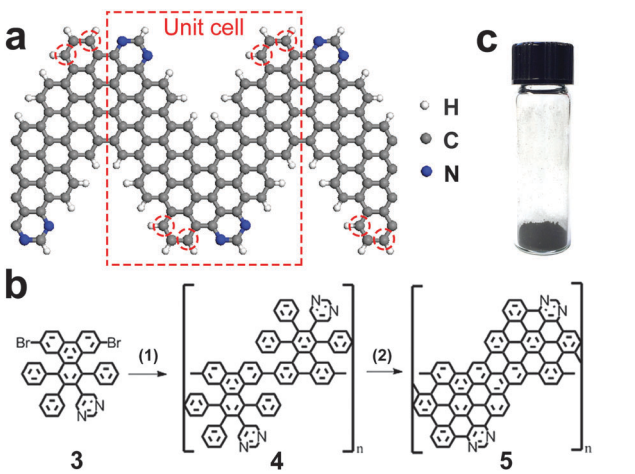

Fig. 1 Synthesis of 4N-GNRs. (a) Schematic of 4N-GNR. (b) Reaction scheme used in this work: (1) Yamamoto coupling, (2) Scholl reaction; see text and ESI† for details. (c) Optical photograph of a 4N-GNR powder.

[a] *Department of Chemistry, University of Nebraska – Lincoln, Lincoln, NE 68588, USA. E-mail: sinitskii@unl.edu*
[b] *Department of Physics, University of Nebraska – Lincoln, Lincoln, NE 68588, USA*
[c] *Department of Physics and Nanoscopy Facility, University of Puerto Rico, PO Box 70377, San Juan, Puerto Rico 00936-8377, USA*
[d] *Department of Chemistry, University of Puerto Rico, PO Box 70377, San Juan, Puerto Rico 00936-8377, USA*
[e] *Nebraska Center for Materials and Nanoscience, University of Nebraska – Lincoln, Lincoln, NE 68588, USA*

† Electronic supplementary information (ESI) available: Experimental details (synthesis and characterization). See DOI: 10.1039/c4cc00885e

of coupling (Fig. 1b), so as the result, the positions of nitrogen atoms in the ribbon edge could vary, *i.e.* the nitrogens could also occupy the positions highlighted with red circles in Fig. 1a instead of the ones shown in the schematic. However, the N : C ratio of 1 : 20 in this ribbon should be the same regardless of how the monomer molecules couple with each other.

The synthesis and characterization of the precursor molecule **3**, as well as the reactions used to convert monomer **3** to polymer **4** to 4N-GNR **5** (Fig. 1b) are described in detail in the ESI.† About 100 mg of 4N-GNRs was obtained in a single reaction (Fig. 1c). Previously, we have demonstrated that a similar procedure could be used to obtain >1 g of chevron-type GNRs (nitrogen-free analogues of 4N-GNRs shown in Fig. 1a) in a single reaction,[21] so we believe that the synthesis of 4N-GNRs could also be scaled up to at least a gram scale. Though not soluble in any solvents that we tried, these ribbons could be suspended by sonication in, for example, toluene or mesitylene, and then deposited on different substrates for microscopic and spectroscopic characterization.

It was previously demonstrated that when chevron-type GNRs are deposited from dispersion to a substrate, they could be found in a form of elongated self-assembled nanostructures, referred to as "GNR nanobelts".[21] These nanobelts are only one carbon atom thick and comprise multiple GNRs arranged in a side-by-side fashion.[21] We deposited 4N-GNRs on a variety of substrates (mica, Au(111), copper TEM grid with ultrathin carbon support film) and observed similar nanobelts. Fig. 2a shows an atomic force microscopy (AFM) image of 4N-GNRs that were dispersed in toluene by sonication, deposited on freshly cleaved mica and dried prior to imaging. Observed in this image are high-aspect-ratio nanobelts that are several μm long. The alignment of 4N-GNR nanobelts likely happens in the contact angle between a droplet of 4N-GNR dispersion and a substrate during the solvent drying. As shown in the height profile measured along the blue line in Fig. 2a, the majority of these nanobelts have heights <5 Å, which corresponds to the thickness of a single layer or graphene (Fig. 2b). In fact, in multiple AFM images we observed only one structure with a thickness (t) larger than 5 Å, which is indicated by the black arrow in Fig. 2a. This structure ($t \sim 1$ nm) is likely a rare stack of 2–3 nanobelts. Fig. 2c shows an STM image of the fragment of a 4N-GNR nanobelt on Au(111), which illustrates the side-by-side arrangement of individual ribbons that are over 40 nm long. As we indicated in the previous study of solution-synthesized chevron-like GNRs, it remains unclear if these nanobelts exist in solution or form directly on a substrate by capillary forces during the solvent evaporation.[21] 4N-GNR nanobelts were also imaged by transmission electron microscopy (TEM), see Fig. 2d and e. The nanobelts found on the TEM grids are 8 to 20 nm wide, which corresponds to 8–12 4N-GNRs arranged in a side-by-side fashion, and up to 1 μm long.

Raman spectroscopy is very sensitive to the disorder (edges and other structural defects, chemical functionalization, *etc.*) in carbon materials,[31] so we used this method to confirm the high structural quality of 4N-GNRs. Fig. 3 shows the Raman spectrum of 4N-GNRs, where in addition to the most intense lines at 1324 and 1600 cm^{-1} that are typically referred to as D and G bands, respectively,[31] a series of smaller peaks around the D and G lines could be observed. This fine structure is a direct result of the low dimensionality of a nanoribbon, and the relative intensities and positions of the lines are characteristic for each specific polycyclic aromatic hydrocarbon (PAH).[32] 4N-GNRs synthesized in this work are structurally close to chevron-like GNRs, so this is not surprising that the Raman spectrum of 4N-GNRs is very similar to that of chevron-like GNRs synthesized by the solution approach.[21] Since disordered carbon materials usually show only broad D and G lines without any fine features, the spectrum shown in Fig. 3 indicates the high structural quality of 4N-GNRs.

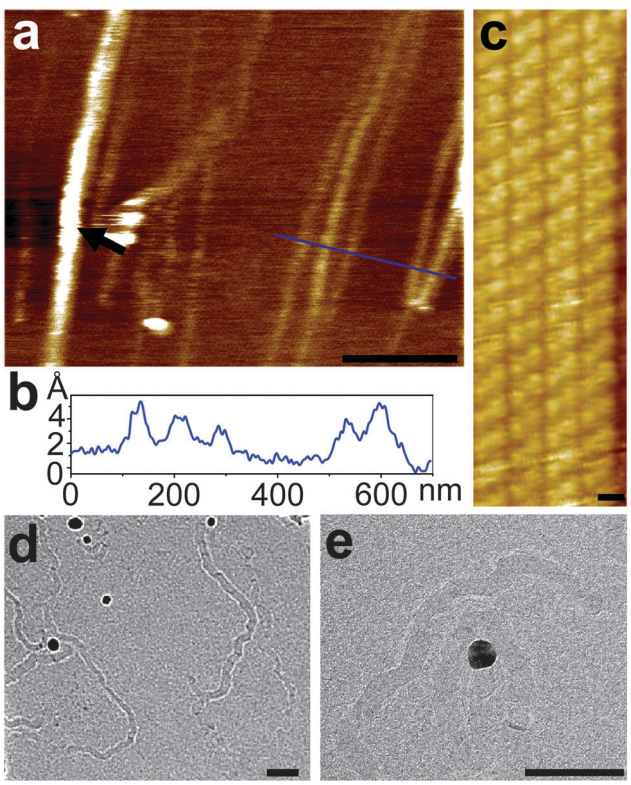

Fig. 2 Microscopic characterization of 4N-GNRs. (a) AFM image of 4N-GNRs deposited on mica. Scale bar is 400 nm. (b) Height profile along the blue line shown in (a). (c) STM image of 4N-GNRs deposited on a Au(111) single crystal. Scale bar is 1 nm. (d, e) TEM images of 4N-GNRs. Scale bars are 50 nm.

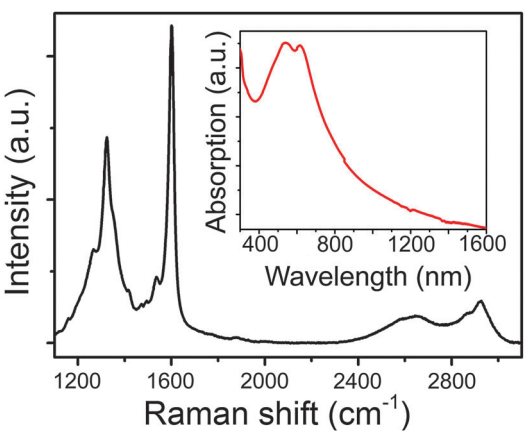

Fig. 3 Raman spectrum of 4N-GNRs. The inset shows UV-vis-NIR absorption spectrum of 4N-GNRs suspended in mesitylene by sonication.

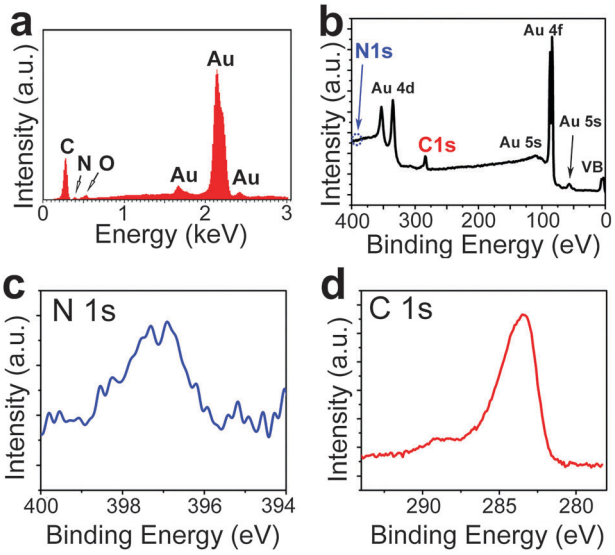

Fig. 4 Spectroscopic characterization of 4N-GNRs. (a) EDX spectrum of 4N-GNRs deposited on a gold substrate. (b–d) XPS spectra of 4N-GNRs deposited on a gold substrate: (b) survey spectrum, (c) N 1s spectrum and (d) C 1s spectrum.

The inset in Fig. 3 shows a UV-vis-NIR absorption spectrum of 4N-GNRs that were suspended in mesitylene by sonication. This spectrum is qualitatively similar to the UV-vis-NIR spectra of other solution-synthesized GNRs, showing a strong absorption in the visible range that gradually decreases with the wavelength increasing toward the infrared region.[19,21] The optical band gap of 4N-GNRs determined from this spectrum is ~1.6 eV.

In order to confirm the presence of nitrogen atoms in the structure of 4N-GNRs we characterized the ribbons by energy-dispersive X-ray (EDX) spectroscopy and X-ray photoelectron spectroscopy (XPS). Fig. 4a shows an EDX spectrum of 4N-GNRs deposited on a gold foil. The nitrogen peak is detectable although small, which is not surprising, considering the expected N : C ratio of 1 : 20. The only foreign peak observed in the spectrum is the low intensity O line, which is likely caused by atmospheric adsorbates. The XPS survey spectrum (Fig. 4b) of the same sample demonstrates only the peaks associated with the GNRs and the gold substrate. XPS N 1s spectrum of 4N-GNRs (Fig. 4c) shows a single peak at 397.1 eV, which is close to pyridinic nitrogen peaks in N-doped graphene.[33] XPS C 1s spectrum (Fig. 4d) contains the main peak corresponding to the C–C bonds and the weaker peak at ~288.5 eV likely representing C–N bonds.[33,34]

In summary, we demonstrate that the synthetic approach based on Yamamoto coupling of N-doped molecular precursors and cyclodehydrogenation *via* Scholl reaction could be used to synthesize high-quality 4N-GNRs. The ribbons were investigated by the combination of microscopic (STM, AFM, TEM) and spectroscopic (UV-vis-NIR, XPS, EDX and Raman spectroscopy) techniques. In the future studies, we will investigate if this approach could also be employed for the synthesis of N-GNRs with other structures and N : C ratios.

This work was supported by the Nebraska Center for Energy Sciences Research (#12-00-13), the Nebraska Research Initiative and the NSF through Nebraska MRSEC (DMR-0820521) and EPSCoR (EPS-1004094).

Notes and references

1 O. V. Yazyev, *Acc. Chem. Res.*, 2013, **46**, 2319–2328.
2 L. Yang, C.-H. Park, Y.-W. Son, M. L. Cohen and S. G. Louie, *Phys. Rev. Lett.*, 2007, **99**, 186801.
3 V. Barone, O. Hod and G. E. Scuseria, *Nano Lett.*, 2006, **6**, 2748–2754.
4 D. A. Areshkin, D. Gunlycke and C. T. White, *Nano Lett.*, 2006, **7**, 204–210.
5 E. R. Mucciolo, A. H. Castro Neto and C. H. Lewenkopf, *Phys. Rev. B*, 2009, **79**, 075407.
6 M. Terrones, A. R. Botello-Méndez, J. Campos-Delgado, F. López-Urías, Y. I. Vega-Cantú, F. J. Rodríguez-Macías, A. L. Elías, E. Muñoz-Sandoval, A. G. Cano-Márquez, J.-C. Charlier and H. Terrones, *Nano Today*, 2010, **5**, 351–372.
7 L. Ma, J. Wang and F. Ding, *ChemPhysChem*, 2013, **14**, 47–54.
8 L. Chen, Y. Hernandez, X. L. Feng and K. Mullen, *Angew. Chem., Int. Ed.*, 2012, **51**, 7640–7654.
9 A. Chuvilin, E. Bichoutskaia, M. C. Gimenez-Lopez, T. W. Chamberlain, G. A. Rance, N. Kuganathan, J. Biskupek, U. Kaiser and A. N. Khlobystov, *Nat. Mater.*, 2011, **10**, 687–692.
10 T. W. Chamberlain, J. Biskupek, G. A. Rance, A. Chuvilin, T. J. Alexander, E. Bichoutskaia, U. Kaiser and A. N. Khlobystov, *ACS Nano*, 2012, **6**, 3943–3953.
11 J. M. Cai, P. Ruffieux, R. Jaafar, M. Bieri, T. Braun, S. Blankenburg, M. Muoth, A. P. Seitsonen, M. Saleh, X. L. Feng, K. Mullen and R. Fasel, *Nature*, 2010, **466**, 470–473.
12 S. Blankenburg, J. M. Cai, P. Ruffieux, R. Jaafar, D. Passerone, X. L. Feng, K. Mullen, R. Fasel and C. A. Pignedoli, *ACS Nano*, 2012, **6**, 2020–2025.
13 Y.-C. Chen, D. G. de Oteyza, Z. Pedramrazi, C. Chen, F. R. Fischer and M. F. Crommie, *ACS Nano*, 2013, **7**, 6123–6128.
14 C. Bronner, S. Stremlau, M. Gille, F. Brauße, A. Haase, S. Hecht and P. Tegeder, *Angew. Chem., Int. Ed.*, 2013, **52**, 4422–4425.
15 J. Sakamoto, J. van Heijst, O. Lukin and A. D. Schluter, *Angew. Chem., Int. Ed.*, 2009, **48**, 1030–1069.
16 X. Y. Yang, X. Dou, A. Rouhanipour, L. J. Zhi, H. J. Rader and K. Mullen, *J. Am. Chem. Soc.*, 2008, **130**, 4216–4217.
17 Y. Fogel, L. Zhi, A. Rouhanipour, D. Andrienko, H. J. Räder and K. Müllen, *Macromolecules*, 2009, **42**, 6878–6884.
18 L. Dossel, L. Gherghel, X. L. Feng and K. Mullen, *Angew. Chem., Int. Ed.*, 2011, **50**, 2540–2543.
19 M. G. Schwab, A. Narita, Y. Hernandez, T. Balandina, K. S. Mali, S. De Feyter, X. L. Feng and K. Mullen, *J. Am. Chem. Soc.*, 2012, **134**, 18169–18172.
20 K. T. Kim, J. W. Lee and W. H. Jo, *Macromol. Chem. Phys.*, 2013, **214**, 2768–2773.
21 T. H. Vo, M. Shekhirev, D. A. Kunkel, M. D. Morton, E. Berglund, L. M. Kong, P. M. Wilson, P. A. Dowben, A. Enders and A. Sinitskii, *Nat. Commun.*, 2014, **5**, 3189.
22 A. Narita, X. Feng, Y. Hernandez, S. A. Jensen, M. Bonn, H. Yang, I. A. Verzhbitskiy, C. Casiraghi, M. R. Hansen, A. H. R. Koch, G. Fytas, O. Ivasenko, B. Li, K. S. Mali, T. Balandina, S. Mahesh, S. De Feyter and K. Mullen, *Nat. Chem.*, 2014, **6**, 126–132.
23 R. Lv and M. Terrones, *Mater. Lett.*, 2012, **78**, 209–218.
24 F. Cervantes-Sodi, G. Csányi, S. Piscanec and A. C. Ferrari, *Phys. Rev. B*, 2008, **77**, 165427.
25 S. S. Yu, W. T. Zheng, Q. B. Wen and Q. Jiang, *Carbon*, 2008, **46**, 537–543.
26 Y. Li, Z. Zhou, P. Shen and Z. Chen, *ACS Nano*, 2009, **3**, 1952–1958.
27 X.-L. Wei, H. Fang, R.-Z. Wang, Y.-P. Chen and J.-X. Zhong, *Appl. Phys. Lett.*, 2011, **99**, 012107.
28 H. Kim, K. Lee, S. I. Woo and Y. Jung, *Phys. Chem. Chem. Phys.*, 2011, **13**, 17505–17510.
29 E. Cruz-Silva, Z. M. Barnett, B. G. Sumpter and V. Meunier, *Phys. Rev. B*, 2011, **83**, 155445.
30 X. H. Zheng, X. L. Wang, T. A. Abtew and Z. Zeng, *J. Phys. Chem. C*, 2010, **114**, 4190–4193.
31 A. C. Ferrari and D. M. Basko, *Nat. Nanotechnol.*, 2013, **8**, 235–246.
32 F. Negri, C. Castiglioni, M. Tommasini and G. Zerbi, *J. Phys. Chem. A*, 2002, **106**, 3306–3317.
33 D. Wei, Y. Liu, Y. Wang, H. Zhang, L. Huang and G. Yu, *Nano Lett.*, 2009, **9**, 1752–1758.
34 A. P. Dementjev, A. de Graaf, M. C. M. van de Sanden, K. I. Maslakov, A. V. Naumkin and A. A. Serov, *Diamond Relat. Mater.*, 2000, **9**, 1904–1907.

Electronic Supplementary Information (ESI) for

Bottom-up solution synthesis of narrow nitrogen-doped graphene nanoribbons

Timothy H. Vo,[a] Mikhail Shekhirev,[a] Donna A. Kunkel,[b] François Orange,[c] Maxime J.-F. Guinel,[c,d] Axel Enders,[b,e] and Alexander Sinitskii*[a,e]

[a]*Department of Chemistry, University of Nebraska – Lincoln, Lincoln, NE 68588, USA*

[b]*Department of Physics, University of Nebraska – Lincoln, Lincoln, NE 68588, USA*

[c]*Department of Physics and Nanoscopy Facility, University of Puerto Rico, PO Box 70377, San Juan, Puerto Rico 00936-8377, USA*

[d]*Department of Chemistry, University of Puerto Rico, PO Box 70377, San Juan, Puerto Rico 00936-8377, USA*

[e]*Nebraska Center for Materials and Nanoscience, University of Nebraska – Lincoln, Lincoln, NE 68588, USA.*

**E-mail: sinitskii@unl.edu*

Materials

Chemicals: Phenanthrene-9,10-dione 95%, potassium hydroxide 85%, diphenyl ether 99% , nitromethane 98%, iron (III) chloride anhydrous 98%, 1,3-diphenylacetone 98+%, phenylacetylene 98+%, copper (I) iodide 98%, N,N'-dimethylforamide were purchased from Alfa Aesar; N-bromosuccinimide 99%, Bis(1,5-cyclooctadiene)nickel(0), cyclooctandiene, triethylamine 99.5%; triphenylphosphine, 2,2'-bipyridyl 99%, toluene 99.5%, and methanol 99.8% were purchased from Sigma-Aldrich; 5-bromopyrimidine 98%, bis(Triphenylphosphine)palladium (II) chloride 98% were purchased from Oakwood Products, Inc.; sulfuric acid 98% was purchased from EMD. All chemicals were used as received without any purification.

Substrates: Mica V4 grade was purchased from SPI Supplies. Gold foils (99.985%) were purchased from Alfa Aesar. Au(111) single crystal (99.999%) for STM was acquired from Princeton Scientific.

Methods

^{1}H and ^{13}C NMRs were performed with Bruker 300MHz, 400MHz and 600MHz NMR instruments. AFM was performed using a Digital Instruments Nanoscope IIIa Dimension 3100 system and Bruker RTESPA AFM probes. All STM measurements were performed using an Omicron low-temperature scanning tunneling microscope with a base pressure of 3×10^{-10} T and an electrochemically etched W tip. UV-vis-NIR measurements were performed using a Jasco V-670 spectrophotometer. EDX analysis was performed using a FEI Nova NanoSEM 450 scanning electron microscope equipped with an Oxford Instruments EDX system. XPS was performed using a PHI Quantera SXM scanning X-ray microprobe. Raman spectrum of GNRs was recorded using a Thermo Scientific DXR Raman Microscope with a 532 nm laser. TEM and electron energy loss spectroscopy (EELS) were performed using a JEOL JEM-2200FS high resolution TEM operated at 200 kV.

Synthesis

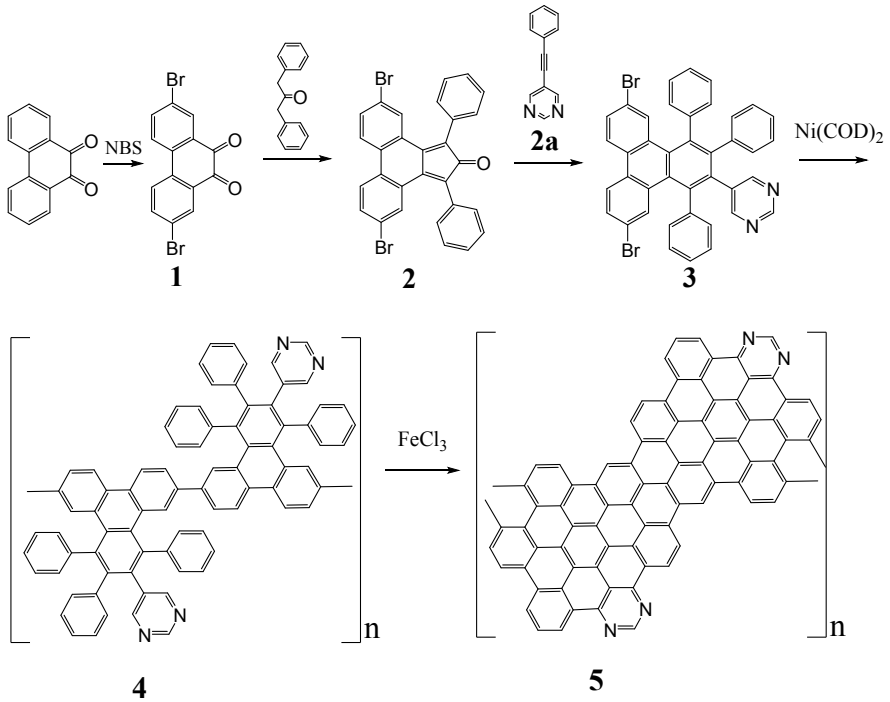

Figure S1. Scheme of the synthesis of 4N-GNRs.

2,7-dibromophenanthrene-9,10-dione (1): 7 g (33 mmol) of phenanthrene-9,10-dione was added to 190 mL of 98% sulfuric acid and followed by the addition of 12.86 g (72 mmol) of NBS. The mixture was agitated at room temperature for 8 h. After stirring, the mixture was added to ice/water bath and filtered to obtain a deep orange solid with a quantitative yield. ^{1}H NMR (300Hz, DMSO-d_6): δ= 8.24 (2H, d), 8.70 (2H, d), 7.95 (2H, dd).

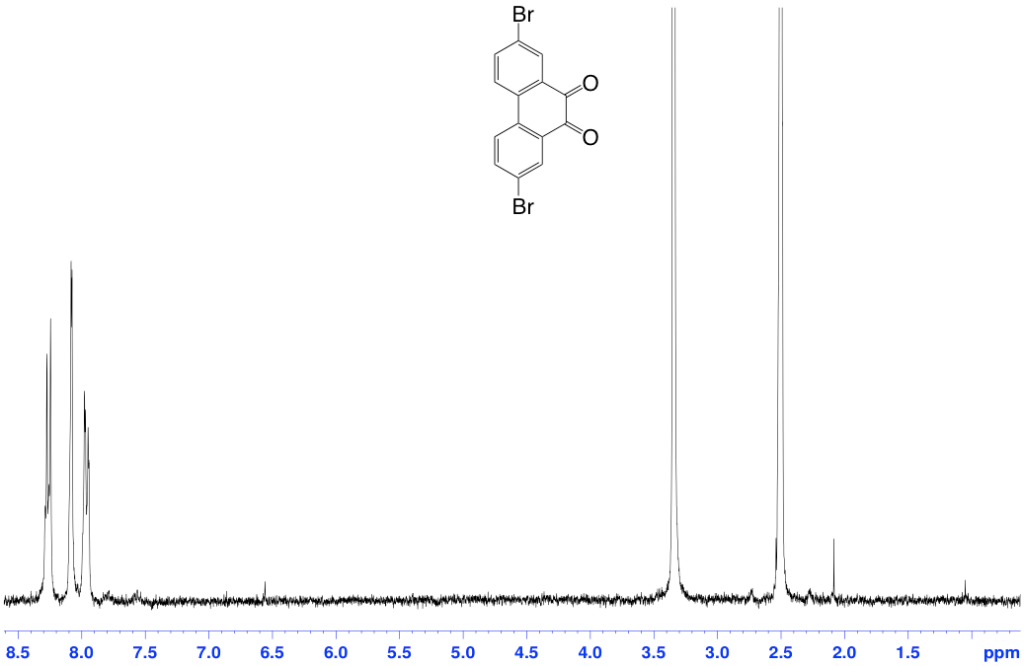

Figure S2. ^{1}H NMR spectrum of 2,7-dibromophenanthrene-9,10-dione in DMSO-d_6.

5,10-dibromo-1,3-diphenyl-2*H*-cyclopenta[*l*]phenanthren-2-one (**2**): 2.67 g (7.3 mmol) of **1** and 1.85 g (8.81 mmol) of 1,3-diphenylacetone were added to 15 mL of methanol under stirring. The reaction mixture was heated to reflux and 25.56 mL solution of 0.3M KOH (7.67 mmol) in methanol was added dropwise. The reaction mixture was refluxed for 2 h and then filtered. 2.5 g of green solid was obtained at 63.4% yield. ^{1}H NMR (600Hz, CD_2Cl_2): δ=7.65 (2H, d), 7.61 (2H, d), 7.49 (4H, dd), 7.45 (2H, dd,), 7.41 (2H, dd), 7.36 (2H, d).

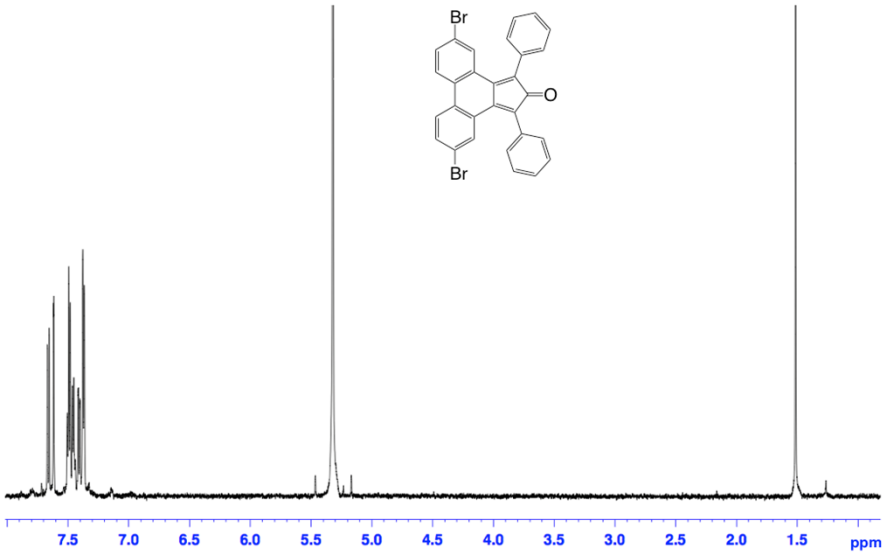

Figure S3. ^{1}H NMR spectrum of 5,10-dibromo-1,3-diphenyl-2*H*-cyclopenta[*l*]phenanthren-2-one in CD_2Cl_2.

5-(phenylethynyl)pyrimidine (2a): 25mL of triethylamine and 25mL of toluene were added to a three-neck round-bottom flask and followed by 2 g (12.57 mmol) of 5-bromopyrimidine, 65.0 mg (0.252mmol) of triphenylphosphine and 120.0 mg (0.629 mmol) of copper iodide. The suspension was degassed using nitrogen for 15 minutes. 441.5 mg (0.6294 mmol) of bis(triphenylphosphine)palladium (II) chloride was added to the reaction flask. The mixture was continued to degas for another 15 minutes and then heated to 60 °C and stirred for 30 minutes. Phenylacetylene (1.70 mL, 15.48 mmol) was added to the reaction flask. The reaction mixture was heated to 65-70 °C for 18 hours. After the stirring period was completed, the side product was filtered off, and the filtrate was concentrated to dryness. The crude product was dissolved in dichloromethane and purified by column chromatography (Ethyl acetate/Hexanes) to obtain 2.076 g of dark amber solid at 92.3% yield. ^{1}H-NMR (300Hz, $CDCl_3$): δ= 9.16 (1H, s), 8.87 (2H, s), 7.57 (2H, m), 7.41 (3H, m). ^{13}C-NMR (300Hz, $CDCl_3$): δ= 158.81, 156.89, 131.97, 129.57, 128.74, 121.97, 120.13, 96.53, 82.47.

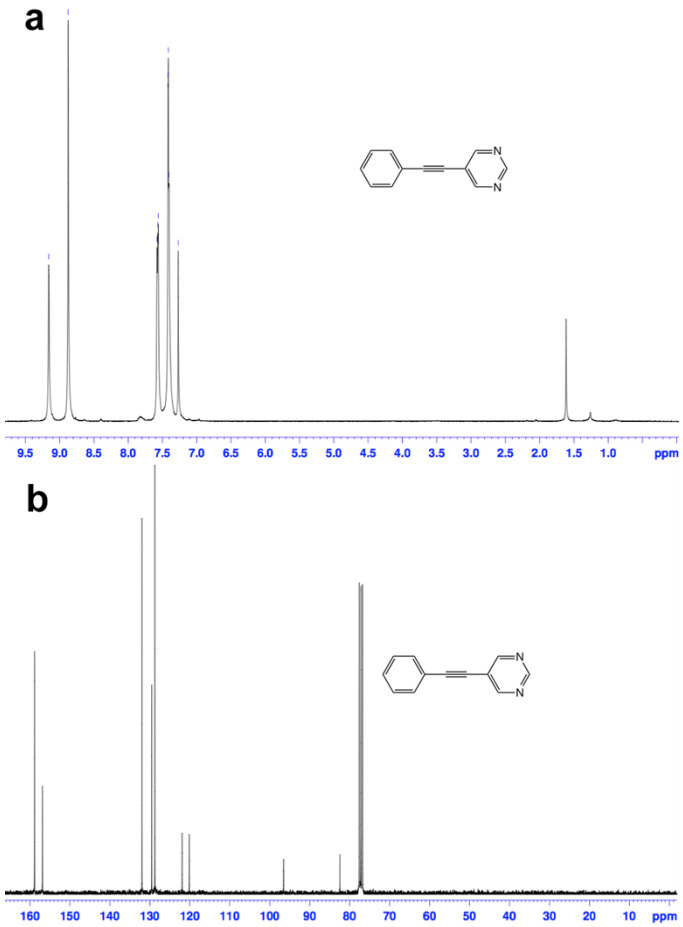

Figure S4. ^{1}H (a) and ^{13}C (b) NMR spectra of 5-(phenylethynyl) pyrimidine in $CDCl_3$.

5-(6,11-dibromo-1,3,4-triphenyltriphenylen-2-yl)pyrimidine (3): To a reaction flask, 5,10-dibromo-1,3-diphenyl-2*H*-cyclopenta[*l*]phenanthren-2-one (**2**) (1.32 g, 2.44 mmol), 5-(phenylethynyl)pyrimidine (**2a**) (0.4 g, 2.2 mmol) and 3 mL of diphenyl ether were added. The reaction mixture was heated to reflux for 24 hours. The reaction mixture was cooled to ambient temperature and purified using column chromatography with hexane and ethyl acetate (90:10) as mobile phase. 0.881 g (57.8% yield) of product was obtained. ^{1}H-NMR (300Hz, $CDCl_3$): δ= 8.78 (1H, s), 8.23 (2H, dd), 8.05 (2H, s), 7.71 (2H, d), 7.53 (2H, d), 7.25 (2H, m), 7.19 (3H, d), 7.04 (8H, m), 6.72 (2H, m); ^{13}C-NMR (300Hz, $CDCl_3$): δ= 158.01, 155.61, 141.49, 141.40, 141.03, 138.83, 138.38, 134.03, 133.18, 132.86, 132.08, 132.04, 131.89, 131.80, 131.60, 130.62, 130.35, 130.27, 129.97, 129.91, 129.34, 128.71, 127.94, 127.75, 127.38, 126.74, 124.83, 124.77, 120.56, 120.52.

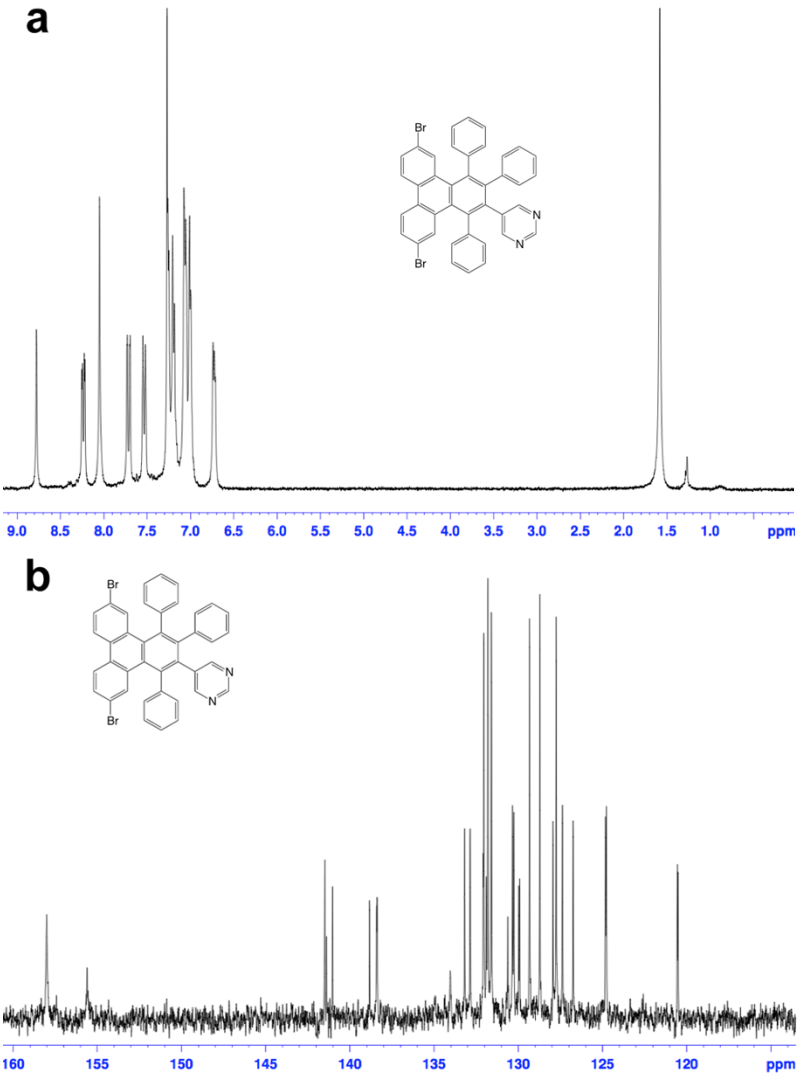

Figure S5. ^{1}H (a) and ^{13}C (b) NMR spectra of 5-(6,11-dibromo-1,3,4-triphenyltriphenylen-2-yl)pyrimidine in $CDCl_3$.

Polymer 4: To a dried and degassed reaction flask, 0.887 g (3.22 mmol) of Bis(cyclooctadiene)nickel was added and followed by a mixture of 2,2'-bipyridyl (0.54 g, 3.22 mmol) and 1,5-cyclooctandiene (0.4 mL, 3.22 mmol) in dried and degassed *N,N*-Dimethylformamide (9 mL). The reaction mixture was heated to 60 °C for 30 minutes. The degassed solution of monomer 3 (0.559 g, 0.81 mmol) in toluene (28 mL) was added to the reaction flask. The reaction mixture was heated to 80 °C for 3 days. The reaction flask was cooled to ambient temperature, and methanol/water mixture (50mL/10mL) was added. The slurry was filtered and washed with methanol, concentrated hydrochloric acid, methanol, sodium hydroxide/methanol solution, water, and hexanes. The solid was dried yielding 0.362 g (84%) of the product.

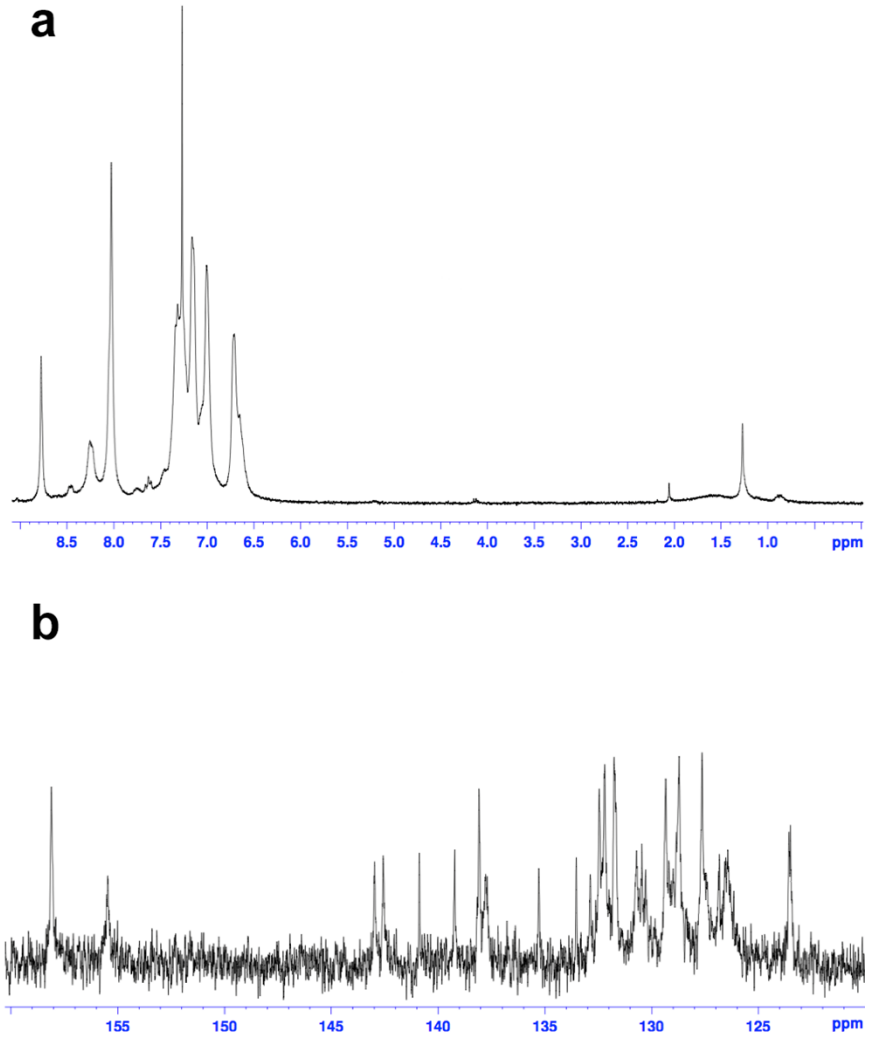

Figure S6. ^{1}H (a) and ^{13}C (b) NMR spectra of polymer **4** in $CDCl_3$

4N-GNR (5): In a reaction flask, 140 mg of polymer **4** and dichloromethane (70mL) were sonicated until all solids were dispersed well. Iron (III) chloride (7 g) was dissolved in nitromethane (8 mL) and then added to the reaction flask. Nitrogen gas was bubbled through the reaction mixture for 15-24 hours while stirring. After the stirring period was completed, ethanol was added. The reaction mixture was filtered and washed with concentrated hydrochloric acid, water, methanol/sodium hydroxide solution, water and methanol. The black solid was dried at 50 °C for 24 hrs. yielding 95.1 mg of black powder.

Sample preparation

Preparation of AFM samples: Approximately 0.3-0.5 mg of 4N-GNR powder and 7-10 mL of toluene were added to a 50 mL round bottom flask, sonicated for 1 min and then heated to reflux. Then the procedure of sonication (30 sec)/reflux was repeated twice. Using a glass pipette, two drops of 4N-GNR dispersion were deposited on the substrates while hot.

Preparation of STM sample: The substrate (Au(111) single crystal) was first cleaned by repeated cycles of Ar ion sputtering and annealing to 875 K. Cleanliness of the Au crystal was checked by STM. The 4N-GNRs dispersion was prepared as described in the 'Preparation of AFM samples' section. The clean Au substrate was removed from the ultra-high vacuum (UHV) chamber and 1-2 drops of 4N-GNR dispersion were deposited and allowed to dry in air for approximately 5 minutes. The Au(111)/4N-GNRs sample was reintroduced to the UHV system and annealed to remove adsorbates and solvent residues. Then the sample was cooled to 77 K for imaging. The annealing-cooling process was repeated with the annealing temperature gradually increasing until graphene ribbons were visible in STM images. The final annealing temperature was approximately 320 K.

Preparation of EDX/XPS samples: Several droplets of 4N-GNR dispersion in dichloromethane were deposited on a gold foil and dried in air.

Preparation of samples for UV-vis-NIR measurements: To prepare the sample for UV-vis-NIR measurements, 0.1 mg of 4N-GNRs **5** was dispersed in 6 mL of mesitylene by sonication for 1 minute at ambient temperature. The mixture was heated to reflux for 10 minutes and then sonicated for additional 30 seconds. Heating and sonication were repeated one more time. The 4N-GNR dispersion was poured to a cuvette while still hot (>100 ^{0}C).

Preparation of HRTEM samples: 4N-GNRs were first dispersed in toluene by sonication. 400 mesh copper TEM grids with an ultrathin carbon support film were dipped in the toluene dispersion of 4N-GNRs and dried in air.

Some foreign particles could be observed in Fig. 2d,e. We analyzed these particles by high resolution TEM and EELS and found that they consist of crystalline TiO_2. No titanium compounds were used at any stage of the synthesis of 4N-GNRs (Fig. S1). Furthermore, the 4N-GNR material was analyzed by EDX and XPS (Fig. 4), and no detectable amount of titanium was found in the sample. Therefore, we believe that those few particles observed in the TEM images in Fig. 2d,e are due to contamination, likely during the TEM sample preparation.